

Ninth Quarterly Progress Report

August 1 through October 31, 1997

NIH Project N01-DC-5-2103

# Speech Processors for Auditory Prostheses

Prepared by

Chris van den Honert, Charles Finley and Blake Wilson

Center for Auditory Prosthesis Research

Research Triangle Institute

Research Triangle Park, NC 27709

---

## Contents

[I. Introduction](#)

[II. Development of the Evoked Potentials Laboratory](#)

[A. Realized and Potential Benefits of EP Recording](#)

[B. Technical Challenges in Recording the EP](#)

[C. Recording Strategies](#)

[D. New Laboratory System](#)

[III. Plans for the Next Quarter](#)

[IV. Acknowledgments](#)

[Appendix 1: Summary of Reporting Activity for this Quarter](#)

---

## I. Introduction

One of the principal objectives of this project is to design, develop, and evaluate speech processors for implantable auditory prostheses. Ideally, the processors will represent the information content of speech in a way that can be perceived by implant patients. Another principal objective is to develop new test materials for the evaluation of speech processors, given the growing number of cochlear implant subjects enjoying levels of performance too high to be sensitively measured by existing tests.

Work in the present quarter included:

- Continued preparation for studies with recipients of bilateral implants, including verification of correct operation of an interface system that the University of Innsbruck and we have developed for simultaneous laboratory control of two Med El receivers. The verification was conducted with a local patient with one Med El implant (subject ME1). He compared speech percepts produced by his speech processor and transcutaneous link, by our laboratory system using the interface for one of the two transmitting antennae, and by our laboratory system using the interface for the other transmitting antenna. The percepts for these various conditions were essentially identical; no difference was heard between the two transmitting antennae.
- Initiation of studies with subject ME2 (October 27 to November 14), who has full insertions of Med El implants on both sides. This patient is visiting us from Germany. Ongoing tests include basic psychophysical measures of

sensitivities to differences in the amplitudes and timing of stimuli delivered to the two implants and evaluation of a wide range of speech processing strategies designed to exploit such sensitivities and/or the additional sites of stimulation supported by two implants. The speech reception tests are being conducted with German-language materials, as the subject's command of English is limited. Additional investigators participating in the studies with ME2 include Stefan Brill from the University of Innsbruck, Sigfrid Soli from the House Ear Institute in Los Angeles, and Joachim Müller from the Julius-Maximilians-Universität in Würzburg, Germany. Stefan Brill is serving as a Guest Co-Investigator and also serving as a translator for the subject. Mr. Brill has made major contributions (along with Otto Peter and Erwin Hochmair) to the development of the interface system and also to the design of the studies with ME2. Sigfrid Soli is a consultant for our project, and will be participating in the studies with ME2 for the week beginning on November 3. Dr. Soli is an internationally recognized authority on binaural processing and on measures of speech reception, for both unilateral and bilateral stimulation. He and Dr. Michael Nilsson, also with the House Ear Institute, incorporated German language test materials into a system they have developed for use in studies of binaural processing and perception. That system, with those incorporated materials, is being used in the studies with ME2. Dr. Müller will participate in the studies for the two weeks beginning on November 3. He also will help with translations for ME2. Dr. Müller was the implanting surgeon for ME2.

- Studies with Ineraid subject SR3 (September 25 to October 1), for additional evoked potential measures and for evaluation of CIS strategies as implemented in the processor system for the new CI24M device (manufactured by Cochlear Pty. Ltd. of Sydney, Australia).
- Studies with Ineraid subject SR10 (October 2-11), for a variety of continued psychophysical, evoked potential, and speech reception measures.
- Ongoing studies with Ineraid subject SR2 (usually one morning per week). Studies in this quarter included (a) psychophysical and electrophysiological measures like those described in Quarterly Progress Reports 7 and 8, but with different stimulus conditions; (b) continued measures of intracochlear EPs with high rate stimuli; and (c) completion of speech reception measures with CIS processors using different numbers of channels and various channel to electrode assignments (most of the remaining conditions involved processors with 1, 2 or 3 channels).
- Presentation of project results in three invited lectures at the 1997 Conference on Implantable Auditory Prostheses (August 17-21) and in one invited lecture at the 28<sup>th</sup> Annual Neural Prosthesis Workshop (October 15-17).
- Continued development of the evoked potentials and speech reception laboratories.
- Continued analysis of speech reception and evoked potential data from prior studies.
- Continued preparation of manuscripts for publication

A highlight of the last quarter was the 1997 Conference on Implantable Auditory Prostheses, held in Pacific Grove, CA, August 17-21. Conferences in this series certainly are among the best in our field. Interactions with colleagues at the 1997 and prior conferences have been invaluable to the project, in that the interactions have helped us refine and improve our work. In some cases, the interactions have helped us chart new directions.

In addition to receiving these benefits, our group offered its own contributions to the 1997 Conference. Charles Finley served as the Co-Chair for the Conference. Blake Wilson, Charles Finley and Dewey Lawson each presented invited lectures. Blake Wilson also served as a discussion leader for a focus group on "issues in speech processor design," and Dewey Lawson also served as a discussion co-leader for a focus group on "binaural stimulation – opportunities and limitations."

In this report we describe the many developments and improvements to the evoked potentials laboratory that have been made during the course of the current project. In broad terms, these developments and improvements have (1) greatly extended the range of studies that can be conducted with recordings of intracochlear evoked potentials and (2) increased the quality of the recordings, which in turn has allowed increases in the rate of data collection for a given signal-to-noise ratio. Results from other studies and activities indicated in the list above, such as results from the studies with bilateral subject ME2, will be presented in future reports.

## **II. Development of the Evoked Potentials Laboratory**

### **A. Realized and Potential Benefits of EP Recording**

Evoked potential recording of intracochlear potentials offers a unique opportunity to examine neurophysiological events in the human cochlea in response to electrical stimulation. Present methods allow observation of responses to single pulsatile stimuli as well as to pairs or long trains of pulses presented at high rates. The latter studies permit examination of temporal integration and neural refractory behavior. By recording from multiple unstimulated electrodes within the cochlea, the spatial distribution of the stimulating electrical fields and the resulting neural responses may be examined. Combinations of these methods permit studies of the spatial and temporal components of channel interactions. Future studies correlating these findings with psychophysical observations and anatomical data on electrode placement and cochlear integrity from advanced cochlear imaging technology promise great advances in understanding of the underlying mechanisms of electrical stimulation in the cochlea. Such understanding will hopefully lead to refined electrode designs and stimulation strategies that will produce better speech understanding for both present and future cochlear implant users.

While much has been learned from these studies to date, it is clear that the present recording methodology is quite limited in its overall performance. Such limitations derive directly from the difficulties in recording small evoked neural potentials in the presence of very large electrical artifacts. Various stimulation /recording protocols using specialized equipment have been developed to overcome these barriers with a good degree of success. However, the fact remains that many of the studies using these methods must necessarily stimulate at levels well in excess of stimulation levels used in speech processors. Consequently, many of the present observations may not reflect the underlying events occurring during actual use of a cochlear implant by a patient. Commonly responses to both positive- and negative-leading stimuli are averaged to reduce the artifact residuals. This produces EP results that do not necessarily reflect the response to either pulse alone but rather to an intermediate variant that is difficult to interpret in the context of known mechanisms of neural electrical stimulation. An additional limitation of the present methods is the the long recording time required to complete the necessary averaging of repeated stimulus trials to extract the low level neural responses from a noisy background. To justify long-term averaging, we commonly assume that the stimulated cochlea is stationary in its responsiveness - an assumption that may or may not be valid. Finally, the spatial resolution of recordings made from unstimulated electrodes is unknown. To date most intracochlear EP recordings have been made from an electrode adjacent to the stimulating electrode. We have little information to indicate if the present recordings truly reflect events occurring closer to the stimulating site.

Recently we have reassessed the requirements of making intracochlear EP recordings, and have invested a substantial engineering effort into design of a second generation of stimulation and recording instrumentation that significantly reduces many of the limitations of past recording methods. This report defines the technical problems and describes new equipment engineered to meet these challenges. The new facilities have afforded substantial improvements in the speed, precision, and resolution of EP recordings in our laboratory. Further on-going developments to extend this work for recording with single-polarity stimuli and/or directly from the stimulating electrode are briefly addressed.

## **B. Technical Challenges in Recording the EP**

The intracochlear evoked potential (EP) is a relatively weak electrical event. Its magnitude depends on many factors including stimulus intensity, repetition rate, neural firing history, and proximity of the recording electrode to the stimulated neurons. Even in response to relatively strong stimuli it rarely exceeds a few hundred microvolts. With stimulus intensities near psychophysical threshold, or at high repetition rates, its magnitude can drop by two orders of magnitude or more. Recording of the EP is complicated by the fact that it is inevitably contaminated by extraneous additive signals. These extraneous signals can be divided into random noise and stimulus-related events. Each of these two types can be further divided into signals of biological origin, and signals generated by the stimulation or recording instrumentation.

### ***1) Noise***

Random noise in the recorded signal arises from five sources: 1) intrinsic noise which includes biological noise generated by background neural or muscular activity, and the thermal noise of the source impedance in the tissue and electrodes; 2) injected noise from the stimulating electronics; 3) noise in the front end of the recording amplifier; 4) output isolator noise; and 5) quantizing noise introduced when the signal is digitized for averaging. In most cases one of these noise sources dominates, and establishes the effective signal to noise ratio.

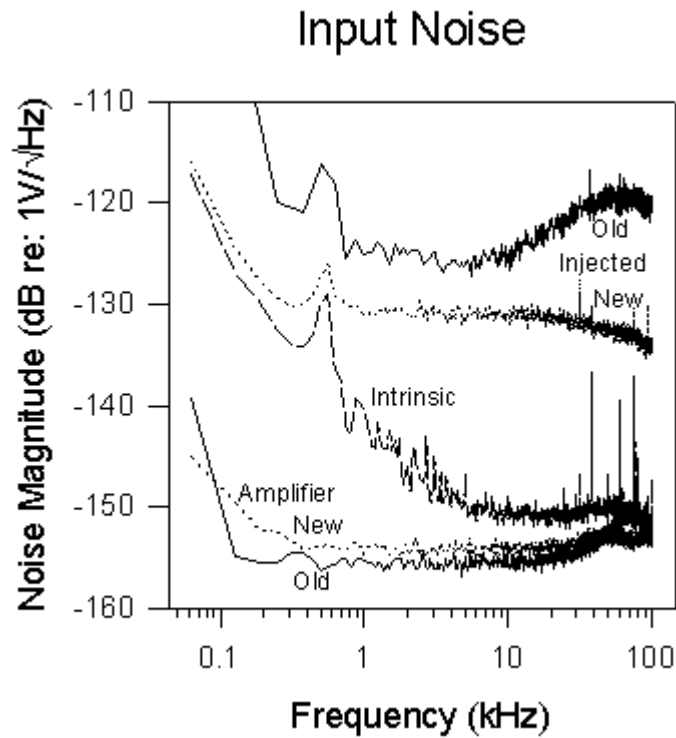
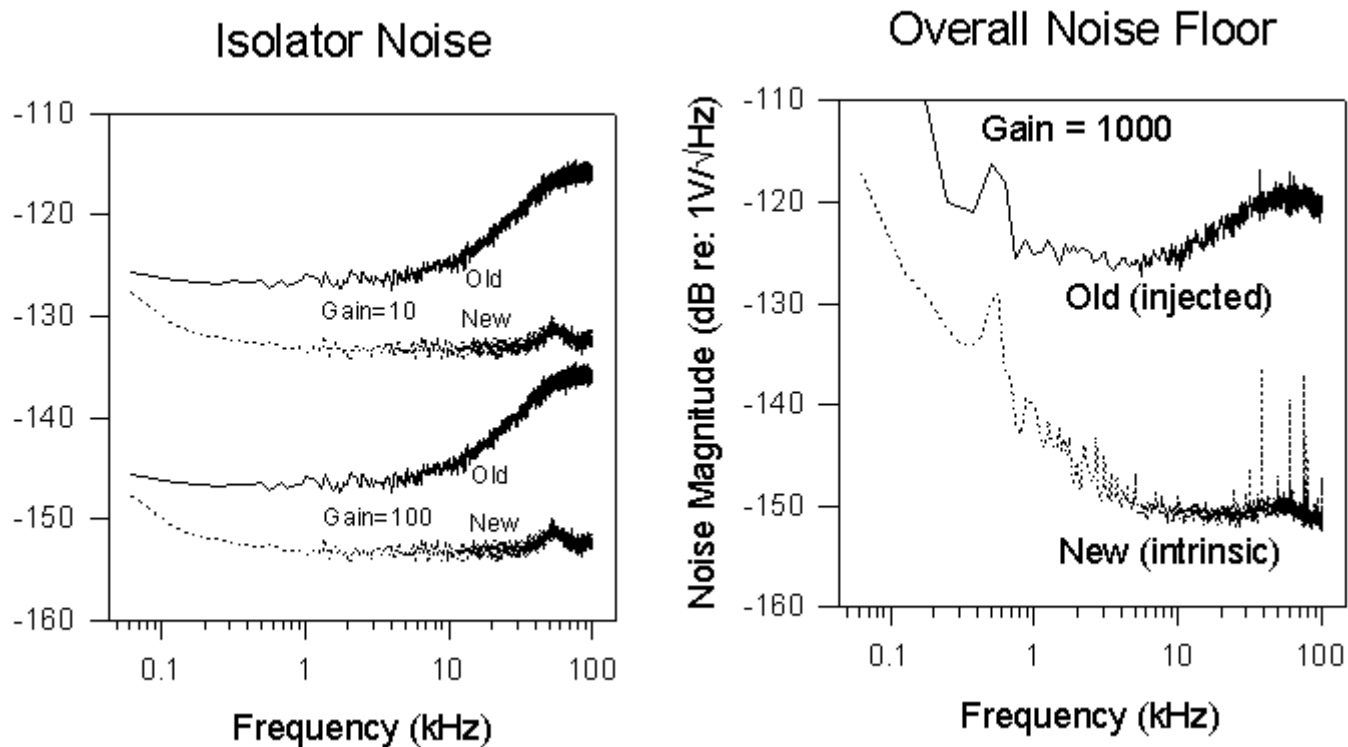


**Figure 1a. System noise spectra, referred to amplifier input.** Injected and amplifier noise floors are shown for the original equipment (solid lines) and the new equipment (dotted lines). The dashed line indicates the intrinsic noise floor measured from electrode 4 of an Ineraid array with respect to the extracochlear ground. Lines above 30 kHz reflect pickup of extraneous sources.

Intrinsic noise is dominated by the biological component whose magnitude drops with increasing frequency, reaching the thermal noise floor of the tissue/electrode source impedance at about 5 kHz. (Figure 1a, dashed line). Injected noise (Fig 1a, top two lines) is due to noise current which flows from the stimulator's electronic circuits through the stimulating electrodes and tissue, even when the stimulus is nominally zero. Such noise is common with the linear current source circuits often used in laboratory environments to provide arbitrary stimulus waveform capability. It typically arises primarily from linear isolation circuits which are used to couple the stimulus waveform signal from line-powered sources. Unlike other noise sources, injected noise varies with proximity of the recording electrode to the stimulating electrode(s). Injected noise generally dominates the recorded noise signal, and determines the overall signal to noise ratio. If the amplifier input stage is well designed, its noise will fall below the intrinsic noise level, and can be ignored. The final two noise sources (isolator and quantizing noise) can often be ignored as well. They are introduced at the end of the recording signal path and are generally small in comparison to the amplified noise from input sources. However when low amplifier gain is used either can become the dominant noise source in the signal as illustrated in Figure 1b. It is sometimes desirable to utilize such low amplifier gains to maintain system linearity for purposes of canceling stimulus artifact (see below).



**Figures 1b,c. System noise spectra, referred to amplifier input. b)** Noise floors for the original (solid lines) and new (dotted lines) linear isolators which couple the EP signal to the line powered equipment. Noise referred to input depends upon the preceding gain. **c)** Overall system noise floors. Noise in the original system (solid line) is limited by injected noise from the current source. The new system (dotted line) is limited by intrinsic noise (see discussion of current-source gating).

Finally, systematic noise can arise from electrostatic or electromagnetic pickup from nearby electrical sources. Examples of these include the power line (60 Hz and its harmonics) and high frequency noise from switching power supplies or video display deflection coils.

Contamination from noise can be reduced effectively with well known signal averaging techniques. The stimulus is presented repeatedly and responses to multiple presentations are averaged. This technique assumes that the EP response is stationary. Although noise can be reduced with signal averaging, this comes at the cost of increased data collection time. The rate at which responses can be collected is limited by the duration of the experimental stimulus itself (which may be hundreds of milliseconds or more) plus the time needed for the nerve fibers to return to rest after stimulation (generally 10 to 20 ms). The number of responses which must be averaged, and hence the time required for a measurement, is proportional to the square of the signal-to-noise improvement required. Consequently reduction of background noise can dramatically increase data collection efficiency.

## 2) Stimulus Related Contaminants

The flow of stimulus current through the tissue produces a three dimensional potential field. The positive and negative recording electrodes register the voltage difference between two points in that field. Thus the passage of a stimulating current pulse produces a voltage pulse across the recording electrodes. That voltage pulse is referred to as the stimulus artifact. (In common usage this term is also used to describe any stimulus-related component of the recorded signal other than the biological response, such as switching transients, electrostatic or electromagnetic pickup, etc.) The magnitude of the stimulus artifact is often 3 to 5 orders of magnitude greater than the biological response to be measured, and is generally greater for monopolar than for bipolar stimuli.

It is customary to utilize brief stimulating current pulses to elicit EPs (although there are exceptions - see below). The intent is to terminate the stimulus current rapidly such that the artifact disappears prior to onset of the biological response. In practice this strategy is only partly successful due to the short latency of EP responses at the intrascalar

recording site and the finite time needed for the artifact signal to subside. The leading edge of the intracochlear EP typically appears within 150  $\mu\text{s}$  of stimulus onset, and the N1 peak generally occurs within 300  $\mu\text{s}$ . For illustration we assume a 30  $\mu\text{s}/\text{phase}$  biphasic stimulus pulse, an EP magnitude of 100  $\mu\text{V}$ , and an artifact magnitude of 1V. If we can accept a 10% perturbation in the magnitude of the EP, then the artifact must settle from 1 V to 10  $\mu\text{V}$  (0.001%, or 100 dB) within the 90  $\mu\text{s}$  following stimulus offset. Within this time, three distinct processes must be completed: 1) the current flowing through the stimulating electrodes must fall by 100 dB; 2) the potential in the tissue between the recording electrodes must fall 100 dB; and 3) the recording amplifier output must fall 100 dB. Only two of these processes (1 and 3) are under control of the circuit designer. Of those two, the recovery speed of the recording amplifier is generally the more problematic.

In order to recover rapidly from the artifact the recording amplifier must have a rapid impulse response which implies correspondingly wide bandwidth. This requirement precludes the use of lowpass filtering to reduce noise. However wide bandwidth does not guarantee rapid settling to 0.001%. Settling time to this level of precision is more often determined not by linear time constants but by nonlinearities in the components (*e.g.* transient heating of IC substrates during the pulse). Much more severe nonlinearity is introduced if the amplifier is overdriven by the artifact pulse, driving semiconductors into saturation. Recovery is then delayed while semiconductors come out of saturation and return to linear operation, at which point the linear recovery trajectory begins. A high gain amplifier (*e.g.* 1000x) can be overdriven by 40 or 50 dB during the artifact, driving many stages into saturation. In this case recovery time is extended as the stages come out of saturation sequentially beginning with the input stage and progressing to the final gain stage. Thus an amplifier which recovers slowly must be operated at lower gain (using fewer gain stages), which exacerbates isolator and quantizing noise effects.

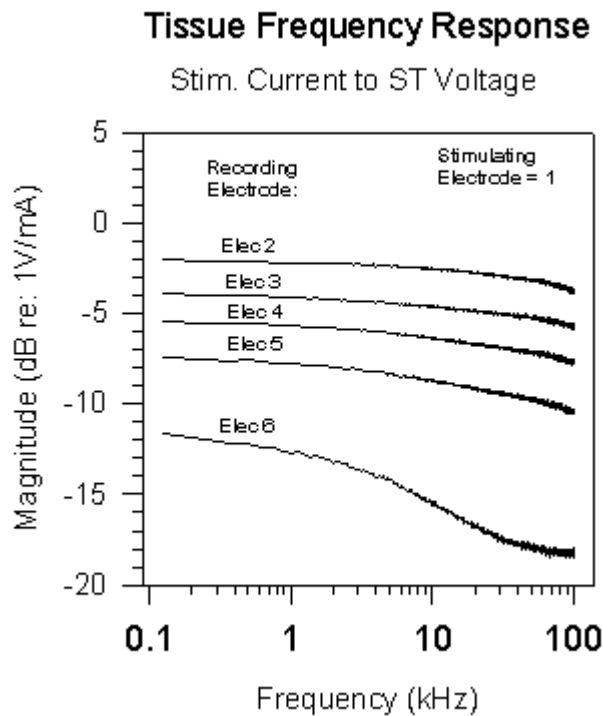


**Figure 2a. Demonstration of tissue reactance.** Frequency response measured with an Ineraid subject. Monopolar broadband pseudorandom noise current was presented through electrode 1 at an audible but low level. Current spectrum was measured from the voltage drop across a 1 kOhm series resistor using the new EP amplifier. Voltage spectra were measured at each of the remaining intracochlear electrodes with respect to the ipsilateral mastoid, using the same amplifier. Voltage spectra were divided by the current spectrum to compute the displayed frequency response magnitude functions.

Assuming for the moment that both the stimulator and amplifier can be designed to recover very rapidly, the time required for the artifact to subside is ultimately limited by the rate at which the potential field within the tissue disappears. If the tissue were purely resistive the field would disappear instantaneously with the cessation of stimulus current flow. Unfortunately the tissue impedance is not purely resistive, but exhibits a small reactive component. This

is illustrated in Figure 2a which shows frequency response functions measured between the stimulus current through the most apical electrode (1) of an Ineraid array and the resulting artifact voltage measured at each of the remaining five electrodes. As expected the artifact voltage response drops off monotonically as the recording site is shifted progressively basalward from electrode 2 to electrode 6. If the tissue were purely resistive the transfer functions would be flat (*i.e.* they would show no frequency dependence). Instead they exhibit a low-pass filter characteristic. Electrode 6 is atypically slow, rolling off 3 dB at 6.25 kHz. The frequency response at the remaining electrodes is relatively wideband, down only 2-3 dB at 100 kHz. Such wide bandwidth would suggest a time constant of only a few microseconds if the tissue behaved as a simple lumped-constant single pole filter. But as Figure 2b demonstrates, this is not the case. The solid curves represent the scala tympani voltage responses to biphasic pulses of each polarity. Following termination of each pulse the recorded voltage falls gradually back to zero, but not with a simple exponential time course. The initial slope (beginning off-scale at 320 mV) exhibits a time constant of only 5  $\mu$ s, which should produce the exponential trajectories indicated by the dotted lines. However the actual recovery is much slower. The "time constant" of the actual trajectory is not a constant at all, but increases monotonically as the voltage drops. As a result a significant stimulus artifact persists into the 1 ms post-stimulus time period in which the EP occurs.

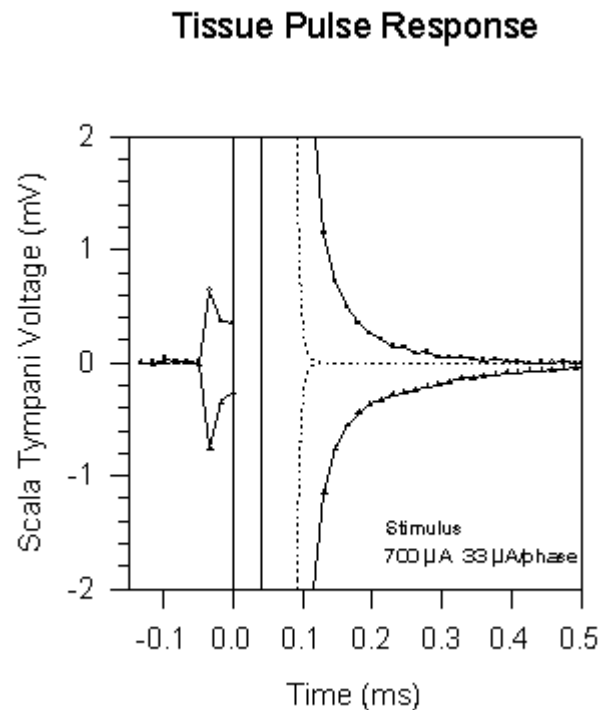


**Figure 2b. Demonstration of tissue reactance.** Tissue pulse response. Biphasic pulses of each polarity (700  $\mu$ A, 33  $\mu$ s/phase) were delivered through electrode 3 of an Ineraid array. The displayed responses (solid lines) were recorded from electrode 4 with an amplifier gain of 10 to prevent clipping or saturation. Dotted lines represent exponential curves of the form  $V = V_0 e^{-t/\tau}$  where  $\tau=5 \mu$ s as fitted to the first two samples of the trailing edge.

In principle there could also be stimulus-related biological contaminants such as EMG from facial nerve stimulation. Although we have occasionally observed such contamination in ABR recordings, this has not proven to be a significant problem in recording intracochlear EPs with respect to the ipsilateral mastoid.

### 3) Baseline Shift

Ideally the recording amplifier should be DC-coupled to eliminate any long low-cut time constant from its impulse response. However DC-coupling of high gain amplifiers is generally not practical because of drifting DC potentials which exist between recording electrodes. Therefore recording amplifiers are generally AC-coupled above some low frequency cutoff. This low-cut filtering can introduce stimulus related perturbations in the signal. Each artifact voltage pulse produces a small residual baseline shift which subsides slowly at the rate of the low-cut time constant (*e.g.* 100 ms). This is of little consequence with a single pulse, but during a high rate stimulus burst those shifts summate,

producing a "ratcheting" baseline excursion which can saturate the amplifier output.

The same problem applies to the stimulator. Most stimulators are necessarily AC-coupled by virtue of the series output capacitor which is used to block any DC current. The time constant of the AC-coupling is the product of the output capacitance and DC output resistance of the current source (*e.g.*  $\tau = 0.1 \mu\text{F} \times 1 \text{ M}\Omega = 100 \text{ ms}$ ). AC-coupling of a perfectly balanced rectangular biphasic pulse results in a tiny current flow following the second phase which decreases exponentially with time constant  $\tau$ . Just as with AC coupling of the amplifier, at high repetition rates these long, late currents can summate to cause "ratcheting" of the artifact baseline.

#### 4) Long Pulse Stimuli

In some cases it is desirable to use stimuli with long pulse widths (*e.g.* for measuring strength-duration curves). This represents a special case because the stimulus artifact cannot be expected to disappear before the appearance of the EP. With very long duration pulses ( $> 500 \mu\text{s}/\text{phase}$ ) the EP may complete before the stimulus does. Under these circumstances the amplifier gain must be reduced to prevent saturation during the pulse, which aggravates isolator and quantizing noise problems. A silver lining to this gain reduction is that current intensities required with such long pulses are somewhat lower, which reduces the magnitude of the artifact accordingly.

### C. Recording Strategies

Depending on the design of the stimulating and recording electronics, artifact recovery speed may be limited by either the instrumentation or the tissue reactance as discussed above. In either case some residual contamination remains which extends into the time interval where the EP occurs. Two methods have been developed for removing the artifact component from the aggregate signal in order to extract the EP waveform. Each involves an arithmetic manipulation intended to cancel the artifact component, and each has advantages and disadvantages.

#### 1) Alternating Polarities

One method for removing the stimulus artifact utilizes biphasic stimuli of alternating initial polarity in the accumulation of the averaged response (Brown and Abbas, *JASA* **88**: 2205, 1990; Finley & Wilson, Abstr. ARO Midwinter Meeting, #711, 1995). The two stimulus polarities produce two responses  $R^+$  and  $R^-$  each consisting of an artifact and an evoked potential:

$$R^+ = A^+ + EP^+$$

$$R^- = A^- + EP^-$$

If inverting the stimulus also inverts the stimulus artifact, then  $A^- = -A^+$ , and the two artifacts cancel each other in the averaged response:

$$R_{\text{AVG}} = 1/2 (R^+ + R^-) = 1/2 \{ (A^+ + EP^+) + (A^- + EP^-) \} = 1/2 (EP^+ + EP^-)$$

The resulting waveform is nominally free of artifact, and consists of the average of the two individual EP responses. This method requires linearity of the tissue to meet the assumption that  $A^- = -A^+$ . This assumption is valid to a good approximation, as shown by the symmetry in Figure 2b. However other factors can limit the validity of this assumption as well. If the amplifier saturates prior to the occurrence of the EP, the recovery from positive and negative saturation must be symmetric. Furthermore any components of the "stimulus artifact" which do not invert with the stimulus current (*e.g.* switching transients or trigger pulse pickup) do not cancel, and will remain in the averaged response.

#### 2) Masking

Brown and colleagues (C.J. Brown, Ph.D. Thesis, Univ. of Iowa, 1989; *JASA* **88**: 2205 1990; *JASA* **88**: 1385, 1990) have described an alternative procedure which uses a template waveform representing the artifact alone with no

biological response component. The template waveform is subtracted from the aggregate response to derive the EP waveform. The template is derived as follows: A composite stimulus is delivered in which the stimulus of interest (the probe) is immediately preceded by a high intensity masker pulse. The purpose of the masker is to excite all of the neurons which would otherwise respond to the probe such that they are in absolute refraction when the probe stimulus occurs. Thus the probe must occur within the absolute refractory period following the masker. The response to this composite stimulus ( $R_{M+P}$ ) includes the artifact of the masker ( $A_M$ ), the evoked potential response to the masker ( $EP_M$ ), and the artifact of the probe ( $A_p$ ):

$$R_{M+P} = A_M + EP_M + A_p$$

The response to the masker alone ( $R_M$ ) is then recorded. This waveform contains only  $A_M$  and  $EP_M$ :

$$R_M = A_M + EP_M$$

Next, the artifact template T (the artifact of the probe only) is extracted by subtracting  $R_M$  from  $R_{M+P}$  as follows:

$$T = R_{M+P} - R_M = (A_M + EP_M + A_p) - (A_M + EP_M) = A_p$$

The response to the probe alone ( $R_p$ ) is then recorded, which contains the artifact of the probe ( $A_p$ ) and the desired EP response to the probe ( $EP_p$ ):

$$R_p = (A_p + EP_p)$$

Finally, template T derived above is subtracted from this response to derive the EP elicited by the probe:

$$\begin{aligned} EP_{\text{DERIVED}} &= R_p - T \\ &= R_p - A_p \\ &= (A_p + EP_p) - A_p \\ &= EP_p \end{aligned}$$

The use of this procedure assumes that: 1) the biological tissue is a linear medium, such that EP and artifact waveforms superimpose; 2) the amplifier is not saturated during the interval of interest containing  $EP_p$ ; and 3) no neurons are excited by the probe when it is preceded by the masker. The third of these assumptions is problematic under some experimental conditions. In anesthetized animals it may be possible to raise the masker intensity to a level which excites every neuron in the cochlea such that none is available to respond to a following probe. In an awake human subject, however, the masker intensity is limited to the maximum comfortable level. The fact that a further increase in intensity generally produces an uncomfortably loud sound suggests that some population of neurons may remain unexcited by the masker. Following the masker pulse these neurons are left in varying degrees of subliminal depolarization. The probe stimulus which follows immediately will excite a fraction of those sensitized neurons through temporal summation. The stronger the probe, the larger that fraction. Thus the probe generates a biological response  $EP_{\text{SUM}}$  (which may be quite small) even when preceded by the masker. This violates assumption (3) above. As a result, the template T is not a pure artifact, but includes the biological signal  $EP_{\text{SUM}}$ :

$$T = R_{M+P} - R_M = (A_M + EP_M + A_p + EP_{\text{SUM}}) - (A_M + EP_M) = A_p + EP_{\text{SUM}}$$

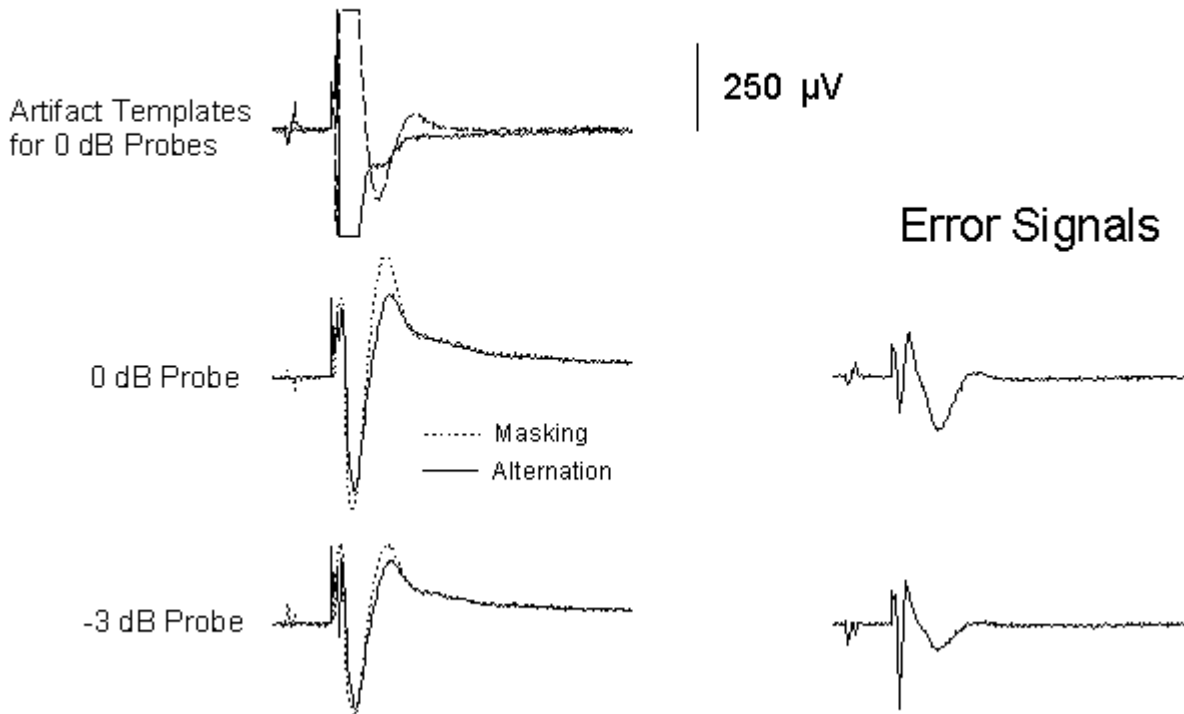
So when the template is subtracted from the probe alone response, the derived EP waveform is altered by the signal

$EP_{SUM}$ :

$$\begin{aligned} EP_{DERIVED} &= R_p - T \\ &= (A_p + EP_p) - T \\ &= (A_p + EP_p) - (A_p + EP_{SUM}) \\ &= EP_p - EP_{SUM} \end{aligned}$$

The magnitude of the summation component  $EP_{SUM}$  depends on the masker and probe intensities. It is minimized when the masker intensity is high (reducing the subliminal population) and the probe intensity is low. Its magnitude increases with probe intensity, and can reach 15% of  $EP_p$  for probe intensities near the masker intensity (Brown and Abbas, *JASA* **88**: 2205, 1990, Figures 1 & 3).

### Masking vs. Alternation



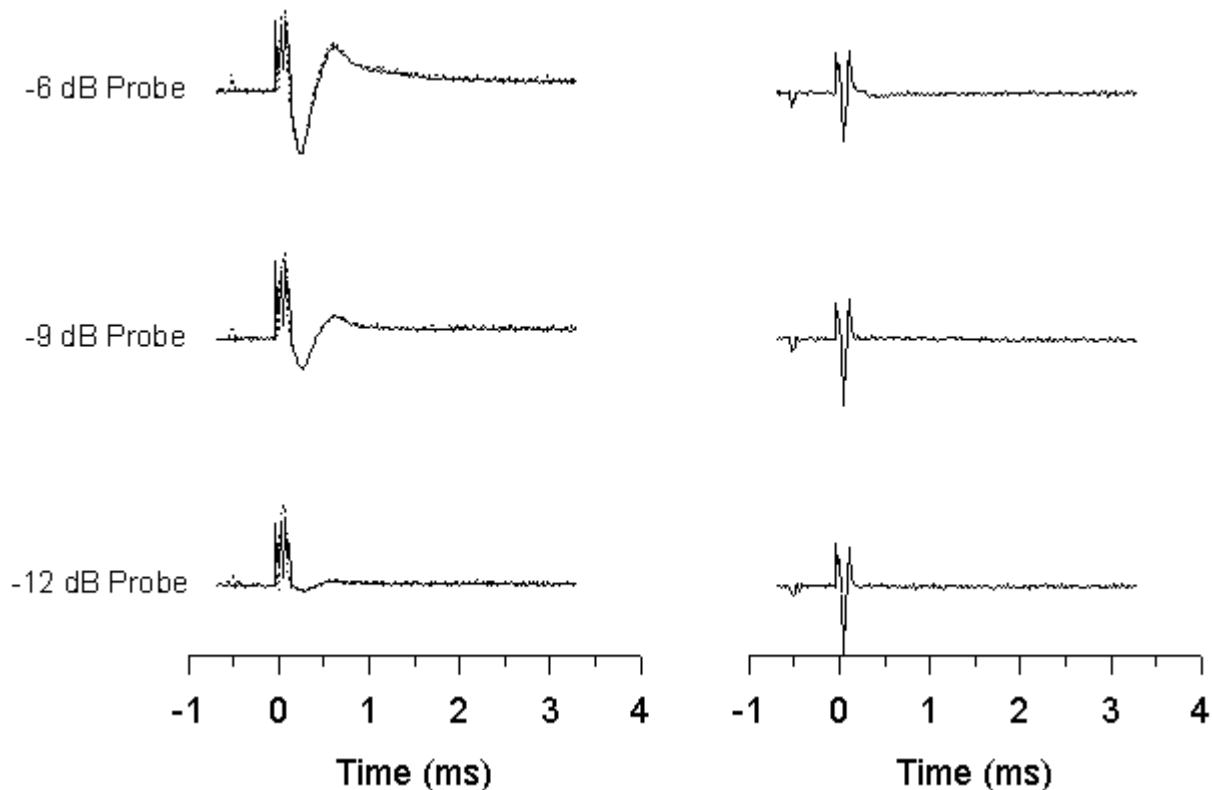


**Figure 3. Comparison of masking and alternation methods of EP measurement.** All stimuli were monopolar 33  $\mu$ s/phase biphasic pulses. Masker level was 1 mA. Probe stimulus onset followed 500  $\mu$ s after masker onset. Stimuli were delivered to electrode 3 of an Ineraid array, and responses were recorded from electrode 4 with respect to the ipsilateral mastoid. The masking paradigm was carried out separately for cathodic-leading (N=25) and anodic-leading (N=25) pulses. The two corresponding artifact templates for the 0 dB probe conditions are shown at the top of the left column. Each dotted trace represents the mean of two masking-derived EPs, one for each polarity. Superimposed solid lines represent alternation-derived EPs (N=50). Each error signal in the right column represents the difference between the adjacent pair of EP traces in the left column.

This phenomenon is illustrated in Figure 3. Intracochlear EP waveforms were measured from the same Ineraid subject using both the masking and alternation methods. The masker intensity was set to the highest current which the subject would tolerate at a rate of 10 pulses/s. Responses were recorded for probe intensities 0, 3, 6, 9, and 12 dB below the masker. The masking procedure was carried out twice for each probe intensity - once for cathodic-leading stimuli, and once for anodic-leading stimuli. The two derived probe responses were averaged together. This mean waveform was compared with the waveform measured using the alternation method with the same two probe polarities.

Derived artifact templates for each of the two 0 dB probes are shown at the top of the left column in Figure 3 (dashed line anodic-first, solid line cathodic-first). The traces have been clipped for display clarity. If the masker is effective in preventing any excitation by the following probe, these templates should be symmetrical and should contain no neural component. But a negative-positive neural component is discernible in each trace, superimposed upon the baseline recovery trajectory. Thus neither template is a "pure" artifact. Each contains a neural summation response evoked by the probe in the wake of the masker.

The consequence of this neural "contamination" of the artifact templates is illustrated in the remaining traces of the left column. For each probe intensity, the alternating-stimulus response (solid line) is compared with the mean of the two masking-derived responses (dotted line). These waveforms should be equivalent. The difference between them represents the error introduced by inclusion of the summation responses in the templates. These differences are plotted as error signals in the corresponding traces of the right column. (Mathematically, each error signal is the mean of the two summation responses.) As expected the error signal becomes negligible when the probe intensity is much smaller than the masker. But for probes of 0 and -3 dB the error is significant in comparison to the responses.

The nature of the distortion by the summation response depends upon its latency and morphology. It is noteworthy that in this case the masking method overestimated the amplitude of the probe response. The summation responses had long latency, and their negative maxima coincided with the late positive wave of the probe responses. Thus when the error signals were subtracted along with the templates, they had the effect of increasing the derived positive wave. However under other circumstances the summation response might act to reduce the derived response. For example if the summation response had the same latency and morphology as the actual corresponding probe response, subtracting it would diminish the magnitude of the derived response. Intermediate summation potential latencies would produce unpredictable distortion of the derived response.

### ***3) Comparison of Methods***

The masking method has two specific advantages in comparison to the alternating polarity method. First, it effectively removes non-invertable components of the stimulus artifact. This can compensate for a wide variety of instrumentation problems such as switching transients from the stimulator or amplifier, asymmetric recovery or other amplifier non-linearities, and spurious pickup. Second, it can be used to measure the individual responses to stimuli of opposite polarity. The stimulated fiber population may change with polarity. And those neurons which are stimulated by both polarities may be excited at different locations along their length when the stimulus is inverted. Therefore the magnitude, latency, and morphology of the EP may vary with polarity. These effects cannot be evaluated using the alternating polarity method.

The masking approach also has disadvantages. As noted above when the masker is submaximal, as is generally the case with human subjects, the derived probe response is distorted by the residual summation component in the artifact template. In addition, the applicability of masking is limited to stimulus trains of fixed amplitude short pulses where a single artifact template is usable for every elicited EP. In contrast masking is not practical for measuring a sequence of EP responses to an amplitude modulated pulse train because in general each pulse would generate an artifact different from the others. It also cannot be used to extract the artifact of a long pulse width probe, because excitation by the probe cannot be confined to the absolute refractory period following a masker. Within the class of fixed intensity trains of short pulses, it is not yet known whether the masking method can be extended to pulse repetition rates where individual artifact waveforms overlap in time. To our knowledge no data are yet available at such rates. A particularly important subset of such stimuli are two-pulse bursts with interpulse intervals  $< 1$  ms which are used to study temporal summation.

In contrast the alternating polarity method can be used with any stimulus waveform. It also provides a marked advantage of efficiency in data collection because fewer stimuli are needed to achieve a particular signal-to-noise ratio. This is true because the target EP response is present in every response collected, whereas with the masking method the target EP is present in only one third of the responses (the probe alone condition). To illustrate this, assume that an acceptable noise level is achieved with 50 presentations using the alternating polarity method. To achieve the same noise level in each of the three waveforms needed for the masking method, a total of 150 stimulus presentations is required. But with each of the subsequent two subtractions the resulting noise level increases (uncorrelated noise powers in the combined waveforms are additive). Thus the noise level in the final derived EP waveform is  $\sqrt{3}$  times greater than in the alternated polarity waveform, even though 3 times as many responses were collected. This phenomenon is illustrated in Figure 4 which replots the -9 dB probe responses of Figure 3 at higher magnification. The noise level of the masking-derived response is greater than that of the alternation trace, even though three times as many stimuli were presented to measure it.

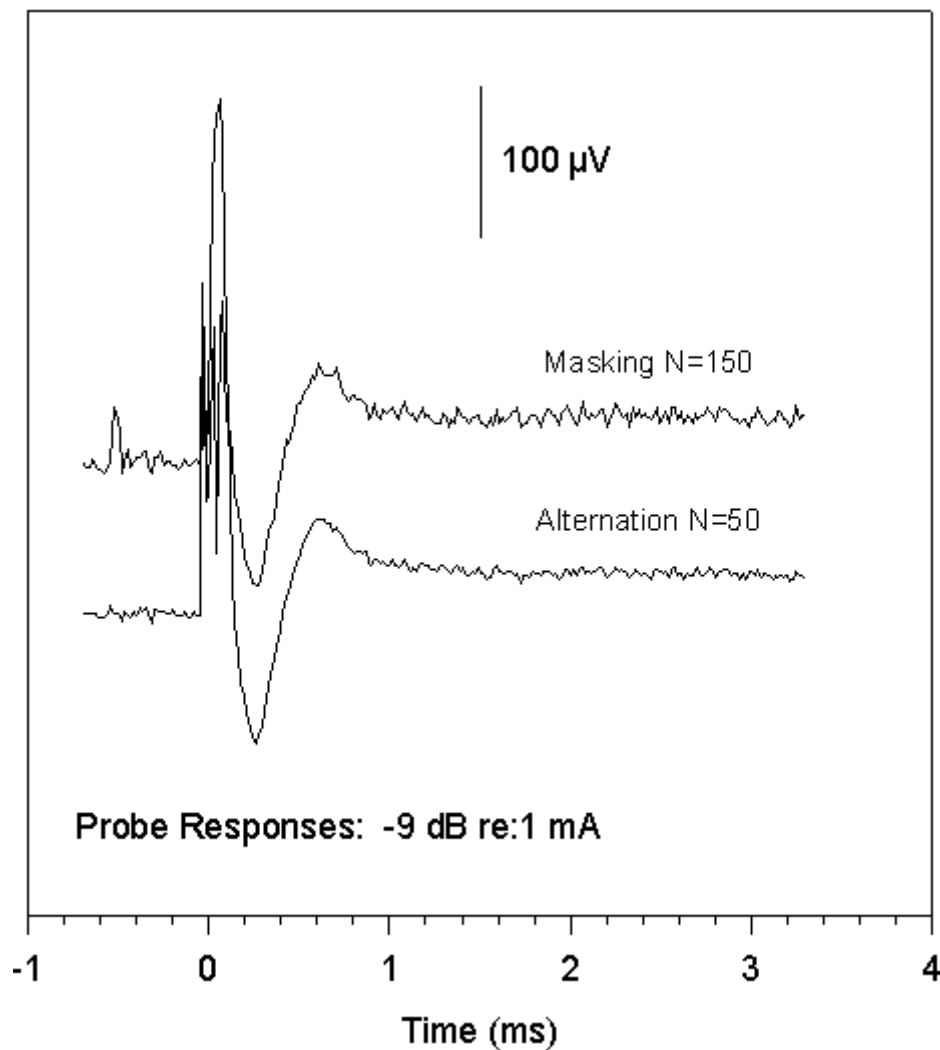


**Figure 4. Comparison of noise levels for alternation and masking methods.** EPs for probe level of -9 dB (re. 1 mA) of Figure 3 are replotted at a higher magnification.

Because it does not reject non-invertable artifact components the alternating polarity places greater demands upon the precision and linearity of stimulating and recording instrumentation. However its primary disadvantage is the inability to resolve the individual responses to stimuli of opposite polarity. We expect that the improved performance of the new instrumentation described below will allow us to implement a new strategy for artifact removal which avoids many of the limitations of the masking method but preserves its ability to measure responses to single polarity stimuli. A discussion of that method follows under Further Advances.

## D. New Laboratory System

### 1) Improved Amplifier Design

#### a) Overload Recovery

It is relatively straightforward to achieve the amplifier bandwidth necessary to produce a rapid step response. However as noted above, high precision settling time is often determined not by linear time constants but by nonlinearities in the circuitry, especially semiconductor saturation. Most high gain amplifiers comprise a cascade of multiple gain stages. A decision was made early in the design process to implement some form of signal clamping at the front end of the signal path which would prevent the artifact from producing saturation of later gain stages. Several approaches were evaluated, including active signal clamping, high speed gain switching, and gating. While each of these was effective in preventing saturation of following stages, all suffered drawbacks. Each of these introduced switching transients, and in some cases recovery speed was only marginally improved due to delays from comparators and/or active clamping circuitry itself. Ultimately a much simpler solution was devised in which each amplifier stage was individually

protected from saturation using back-to-back high speed switching diodes at the input. Two other design decisions made this possible. The first was the implementation of a DC nulling servo loop at the amplifier front end (see below). This avoided the need to clamp around an arbitrary baseline reference value tracked by active circuitry. Second, the maximum design gain of 10,000 was divided among four low gain (10x) stages, with gain controlled by analog routing switches which bypass unneeded stages. A passive diode clamp at the input of each stage permits it to operate linearly up to an output level of about 5 V, but prevents any stage from saturating. At a gain of 1000 the amplifier recovers from a 1 V artifact pulse to 10  $\mu$ V (referred to input) in 10  $\mu$ s.

#### *b) DC coupling*

DC coupling of the amplifier was desired to eliminate the low cut time constant from the impulse response. In order to avoid baseline wander and saturation at high gain due to drifting DC potentials from the electrodes, an integrating servo circuit was implemented which automatically nulls the DC output of the front end instrumentation amplifier. Mathematically this is equivalent to a single-pole high pass filter (ordinary AC coupling). It differs from a filter in that the integrator can be momentarily frozen during delivery of a burst of stimuli. This preserves the advantage of DC coupling by preventing baseline ratcheting during a high rate stimulus burst, but still permits operation with high gain. The integrator is re-enabled after each stimulus burst and resumes nulling of the input offset signal.

#### *c) Isolator Bandwidth/Noise*

The isolator which couples the EP signal from the amplifier to the analog-to-digital converter has traditionally been a weak link in the signal path. Linear isolators are generally slow or noisy or both. Two types of linear isolator are available commercially. Optical isolators use an LED/photodiode combination to couple the signal across the isolation barrier. Full power bandwidth of typical commercial optical isolators is limited by slew rate to 5-10 kHz. Faradic isolators use very small capacitors to transmit a high frequency carrier signal across the isolation barrier. The carrier is modulated by the signal of interest (usually using duty-cycle modulation) which is recovered by demodulation on the output side. Faradic isolators offer higher slew rates but at the expense of poorer isolation and greater output noise. Noise in Faradic isolators is dominated by residual ripple from the high frequency carrier.

A custom optical isolator was developed for the new EP amplifier which provides a 10-fold increase in speed and a 10-fold reduction in peak noise over the component used in our original design. The new isolator utilizes custom linearizing circuitry around a bare LED/photodiode package. This design provides a full power bandwidth of 500 kHz at unity gain with output noise (3 mV p-p) 76 dB below the maximum output signal level. In comparison the Burr Brown ISO150 used in our original design has a bandwidth of 50 kHz and peak output ripple noise 56 dB below the maximum output level. Figure 1b compares the noise floors (referred to amplifier input) of the old and new isolators. The quieter isolator allows us to operate with amplifier gain as low as 100 with no compromise in the overall signal-to-noise ratio.

#### *d) Analog Subtraction Capability*

When the stimulus duration is short, the input clipping described above permits use of high gain by allowing rapid recovery from overload before EP onset. However if the stimulus duration is long such that it spans the time period where the EP occurs, the amplifier must remain in linear operation throughout the pulse - *i.e.* overload clipping must be avoided entirely. As discussed above, this has previously required the use of low amplifier gain with the incumbent noise problems. In order to permit operating at high gain without clipping during a long pulse, an analog template subtraction capability has been designed into the new EP amplifier. Each amplifier has on board two 12-bit digital-to-analog converters which can be used to synthesize template waveforms. Either DAC output can be subtracted from the analog signal at any of the stages in the amplifier chain. This capability will permit subtraction of an approximate artifact template waveform from the input stage signal which in turn permits higher subsequent gain without clipping. The approximate artifact template can be synthesized mathematically or measured with subthreshold stimulus intensities where no EP is elicited. The residual transient artifact will be removed with the same techniques used for short-pulse artifact handling. This hardware capability has not yet been exercised.

#### *e) Current Status*

A prototype breadboard (excluding template subtraction DACs) has been in use in the laboratory for several months.

The design has been entered into schematic capture software, and printed circuit board layout is in progress. At least 8 channels of amplification will be implemented for parallel recording from multiple electrodes.

## 2) *New Stimulator Design*

### a) *Short Pulse Capability*

Emerging CIS processor designs operate at frame rates up to 10 kHz. For a six-channel processor this produces an aggregate rate of 60 kHz, which corresponds to 16.7  $\mu$ s per biphasic pulse, or 8.3  $\mu$ s/phase. A primary goal of the stimulator redesign was to permit operation with phase durations down to 5  $\mu$ s while preserving the ability to deliver arbitrary current waveforms. This requirement imposed several design requirements.

#### **Bandwidth**

One rule of thumb is to require a low-pass time constant no greater than 1/10 of the phase width, which implies a bandwidth of at least 300 kHz ( $\tau = 0.5 \mu$ s;  $f = 1/(2\pi \tau) = 318$  kHz). Since linear isolators with such bandwidths have not been previously available, this requirement has been met in the past by coupling the desired waveform across the isolation barrier digitally, and including a D/A converter on the isolated side (4th QPR, N01-DC-5-2103, May-July 1996). While this is effective, it increases complexity and power consumption of the isolated (battery powered) circuitry. It also increases isolation barrier capacitance. The custom wideband linear isolator described above has been incorporated into the new current source design as well as the recording amplifier. It provides sufficient bandwidth and retains advantages of low barrier capacitance and low power consumption.

#### **Push/Pull Outputs**

When short pulse durations are used, greater current levels are required to achieve approximately equal stimulus intensity. This in turn requires that the stimulator be capable of generating higher voltages across the stimulating electrodes. In our previous stimulator design the load impedance was placed in the feedback loop of an operational amplifier. With this traditional "floating load" design the voltage which can be developed across a pair of stimulating electrodes is limited by the amplifier output excursion from ground ( $\pm 15$  V in our case). In the new design each stimulating electrode (including the extracochlear return) is connected to a dedicated single-ended current source. The algebraic sum of all current source outputs must be zero. In a typical case when stimulating through two electrodes, one output sources current and the other sinks an equal amount. The new output stages operate from  $\pm 30$  V power supplies. As a result, the voltage at any individual electrode (with respect to ground) can reach  $\pm 28$  V, and  $\pm 56$  V can be developed across a pair of electrodes.

The old "floating load" design is also susceptible to stimulus leakage through imperfect isolation barrier capacitance. This is because only the current returning through the "virtual ground" electrode connected to the op-amp input is regulated. Current through the other electrode (connected to the op-amp output) is not explicitly regulated. It is assumed equal to the returning current simply because there is no other pathway back to ground. This is true if the isolation is perfect, but in practice additional current can flow through the unregulated electrode and return to ground through parasitic capacitances including the isolation barrier. The relative significance of this leakage component grows as the current pulses become faster. The new design prevents this phenomenon by explicitly regulating the current flow through every stimulating electrode.

#### **Guarding**

Short stimulus current pulses are subject to another form of leakage as well: leakage across parasitic capacitance in the cabling which couples the stimulator to the subject. This capacitance forms a shunt across the load impedance. The result is low-pass filtering of the current waveform actually reaching the tissue. The time constant of this low-pass filter is determined by the product of the load impedance and the stray capacitance. With a typical 5 kOhm electrode impedance, the 300 kHz desired bandwidth limit is reached with only 100 pF of cable capacitance; with a 20 kOhm electrode impedance only 25 pF is permissible. Such limits are difficult to meet with practical cable lengths and pathways. In order to avoid this problem the new stimulator incorporates shielded outputs coupled through coaxial cables. The shield of each output is not grounded, but is driven by a guard amplifier to be equipotential with the connected electrode. Leakage currents from cable to cable flow from the low impedance guard amplifiers rather than

being bled off from the stimulus current. The guard shields will be extended at least as far as the junction box which accepts the coupling cable to the subject's percutaneous connector. If necessary the coupling cable itself can be replaced with shielded conductors to carry the guarding up to the pedestal.

### *b) Gating*

As noted above in order for the stimulus artifact to become acceptably small prior to the onset of the EP, the actual output current must fall to 0.001% (a factor of 100,000) within the 90  $\mu$ s following stimulus offset. For example, following a 500  $\mu$ A pulse the current must fall to 5 nA during this interval. This imposes a severe settling time constraint on the entire stimulus signal pathway (DAC, isolator, and output stage). An alternative way to guarantee that the current stops rapidly is to interpose an electronic gating switch between the stimulator and the electrode. The switch can be opened by a logic signal at the instant when the pulse is to end.

During early stages of the redesign commercial analog switches were evaluated for this purpose. These components use field-effect-transistors which typically toggle from a few ohms to many Gigaohms of resistance within a fraction of microsecond. They were found to be very effective in interrupting the output current virtually instantaneously. However two difficulties were encountered with these prototypes. The first was the well-known "charge dump" phenomenon. When the switch opens, the control signal at the gate of the FET slews through a large step ( $\sim$ 30V). That rapid voltage step causes a momentary current spike to flow across the parasitic gate-to-source capacitance and into the load (*i.e.* the electrode). This current spike is effectively a secondary stimulus pulse which is brief, but significant. In some cases it produced an artifact as severe as the trailing edge of the original unswitched pulse. This transient does not invert with stimulus polarity and so cannot be removed with the alternation method of artifact cancellation. The second problem was a practical one. We were unable to identify any commercial analog switches which would accommodate the  $\pm$ 30 V range of the output stage power supplies.

Both of these limitations were eventually overcome by substituting an optically controlled FET switch in place of the ordinary analog switch. The FET in this component is floating - not referenced to ground. Its gate-to-source control voltage is developed by an internal photodiode which is illuminated by an electrically isolated light emitting diode (LED) in the same package. Interrupting current through the LED extinguishes the illumination and causes the FET to open. This switch is slower than its electrically controlled counterparts: it requires approximately 20  $\mu$ s to change states. However it produces no charge dump artifact, and can sustain voltages of 300 V in either direction across the switch terminals in the open circuit condition. An additional benefit afforded by this component is that the control signal (the LED current) can be generated by line powered equipment (*viz.* the computer) because it is electrically independent of the switch itself.

When the optical switch opens the current source becomes unloaded. This is generally an undesirable condition because the output stage may become unstable operating into an open circuit. In order to maintain a load on the current source, a dummy load is connected by a second optical switch which closes when the first one opens.

### *c) Injected Noise*

Due to the quieter new isolator, injected noise from the new current source is lower than that of the old design (Figure 1a, top two traces). However it is still greater than the other noise sources in the system. A second and equally important function of the optical gating switch described above is to interrupt the noise current from the stimulator when the stimulus is off. When the switch is opened, the injected noise is eliminated entirely. Thus the overall system noise level is now limited exclusively by intrinsic noise for amplifier gains of 100 or greater. The result is a dramatic reduction in the number of sweeps which must be averaged to achieve equivalent signal quality. The noise improvements of the new current sources are illustrated in Figure 5. The top two traces in the left column illustrate EP responses recorded using the new equipment with the gating disabled. Due to the low injected noise of the new current source, a recognizable EP can be identified with just 2 sweeps (1 of each polarity). But the more dramatic gain is realized when the gating is enabled to remove the injected noise entirely, as shown in the corresponding traces of the right column. For comparison, a comparable record collected with the original equipment using 404 sweeps is shown at the bottom of the right column.

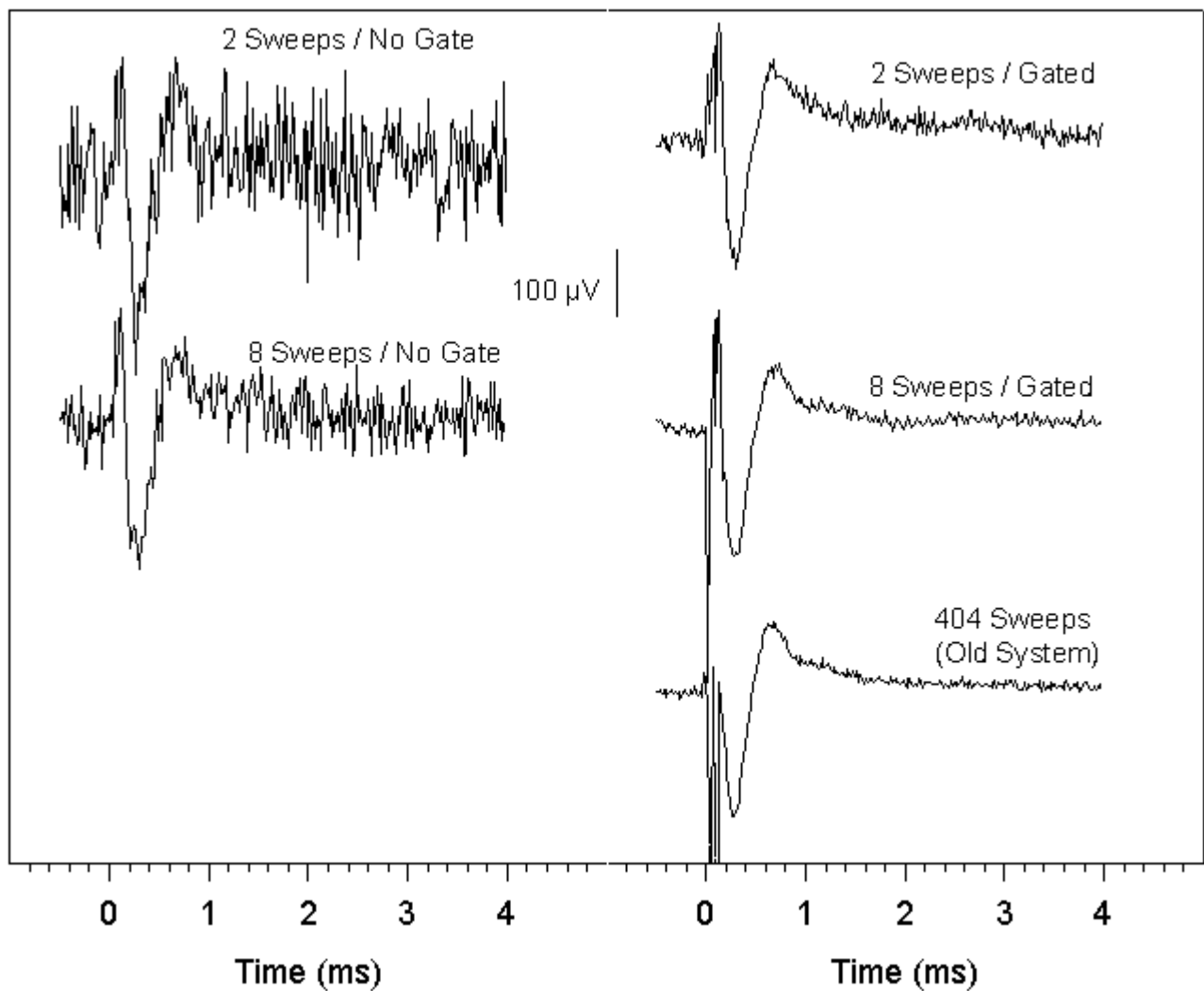


**Figure 5. Injected noise of new current source.** Stimuli were monopolar  $33 \mu\text{s}/\text{phase}$  biphasic pulses at  $500 \mu\text{A}$  delivered through electrode 3 of an Ineraid array. The two EPs in the left column were recorded from electrode 4 with the stimulator output gating disabled, showing the resulting injected noise level for averages of  $N=2$  and  $N=8$ . Amplifier gain = 1000. Corresponding EPs in the right column were recorded with the gating enabled, revealing the underlying intrinsic noise. For comparison an historical recording collected with the original equipment using the same two electrodes ( $I=440 \mu\text{A}$ ,  $N=404$ ) is shown at the bottom of the right column.

#### d) Safety Features

New safety features have been designed into the new stimulators in addition to the electromechanical relays under control of the operator and subject "panic switches." Each current source detects two error conditions: 1) saturation and 2) charge limit. If either error is detected, a global error signal is asserted which causes all of the optical switches (on all of the current sources) to open, disconnecting the subject from all current sources within  $20 \mu\text{s}$ . When an error condition has caused the optical switches to open, they can only be closed again by manual intervention of the operator.

A saturation error occurs whenever the output stage amplifier approaches either power supply rail. The threshold is adjusted such that the error condition is flagged before the amplifier output clips. Saturation errors are most often due to a bad connection between the current source and the load (*e.g.* a bad cable, or a loose connection). With the older "floating load" stimulators a bad connection to the electrodes was relatively benign, because it would completely interrupt the stimulus. With the new system this is not necessarily the case. When a bipolar stimulus is delivered, the two intracochlear electrodes are driven with equal and opposite currents, each by a different current source. If only one of the connections were to fail, the remaining electrode would continue to receive current, which would return through the subject ground instead of the other intracochlear electrode. The stimulus would thus become suddenly monopolar at an intensity intended for bipolar stimulation which might well be uncomfortably loud. For this reason saturation of any

current source triggers an error which interrupts stimulation on all sources.

A charge error occurs if the input signal to a current source would result in delivery of more than 250 nC without a current reversal. This mechanism is not intended to protect against chronic stimulation with unsafe charge densities. (Pulse amplitudes and durations are selected to observe appropriate limits). Instead it protects against failures of the stimulus signal source which would result in anomalous stimulus waveforms. For example if a hardware or software failure prevented timely updating of a stimulus DAC output, a stimulus pulse might be extended to an inappropriate duration (or even indefinitely) resulting in an uncomfortable stimulus. The charge error circuit will detect such a signal anomaly and immediately open all of the optical switches.

#### *e) Current Status*

A prototype breadboard with four current sources (excluding new safety circuits) has been in use for several months. The entire design (including safety circuits) has been implemented on printed circuit boards, and has been completely tested. Each board contains two current sources. Five boards have been populated, and one assembled into a module. The remaining modules and subrack to house them are under construction. An integrated power supply and battery management system (for both stimulators and amplifiers) has been fabricated and tested.

### **3) Further Advances**

#### *a) Single-Polarity Recordings*

As noted above, the neural response to a biphasic stimulus pulse may vary with leading-phase polarity. Both the spatial distribution of excited fibers and sites of spike initiation along the fibers may change when the stimulus is inverted, with concomitant changes in the latency and morphology of the EP components. Therefore it is of interest to measure these responses individually. Although the masking method permits such measurements, it suffers distortion from the neural error signal in the artifact template (Figure 3, right column). In order to avoid this source of error we have adopted an alternate method for defining an artifact template. An artifact waveform is recorded with a low intensity stimulus (preferably below psychophysical threshold) where there is little or no biological response. As a guard against any residual biological component, artifacts with both polarities are recorded and their difference computed to generate the template. This procedure cancels any common-mode components and sums the artifacts. (This is the logical inverse of alternation, which cancels artifact and extracts the common-mode EP by adding traces of opposite polarity stimuli.) In order to generate a template which is appropriate for the higher level stimuli (those used to evoke an EP) the template is scaled up accordingly. For example, if the template is recorded with a 100  $\mu$ A stimulus and the EP is evoked with a 400 $\mu$ A stimulus, the artifact is scaled by a factor of 4 before being subtracted from the averaged waveform.

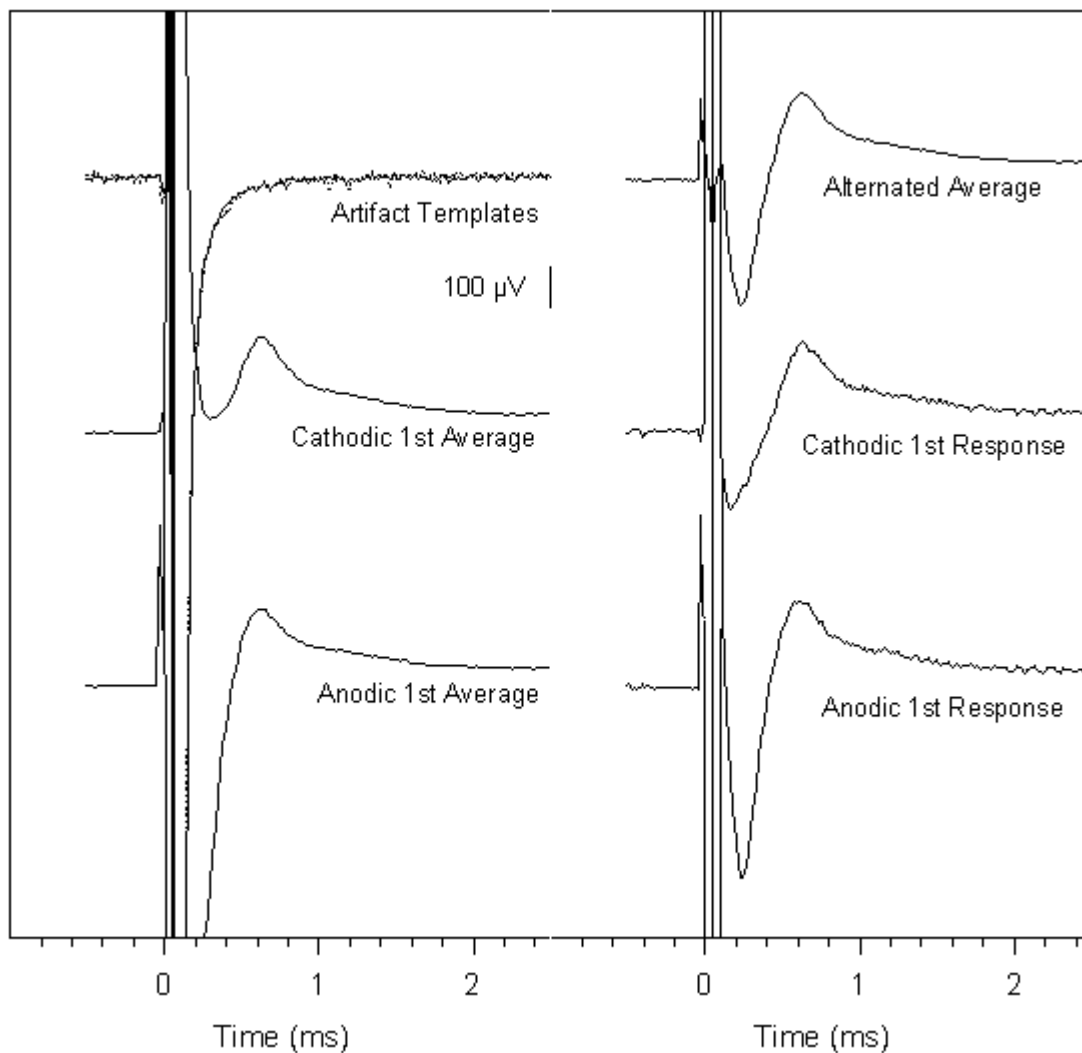


**Figure 6. Responses to single polarity stimuli.** Stimuli were monopolar 33  $\mu\text{s}$ /phases pulses at 812.5  $\mu\text{A}$ . *Left column:* Averaged responses to cathodic-first and anodic-first stimuli at 812.5  $\mu\text{A}$  ( $N=100$  for each). Superimposed traces at the top show artifact templates measured with stimuli of 100  $\mu\text{A}$  (dotted line) and 200  $\mu\text{A}$  (100 cathodic-first and 100 anodic-first each). Templates have been scaled by 8.125 and 4.0625 respectively to match the current intensity used for EP recordings. *Right column:* The top trace shows the usual alternated response computed by averaging the two responses in the left column. The remaining two traces show individual responses to the two stimulus polarities computed by correcting each of the raw averages in the left column with the 200  $\mu\text{A}$  artifact template. The template was subtracted from the anodic-first average, and added to the cathodic-first average.

Figure 6 shows preliminary data which indicate that this method is effective. Separate averaged responses were measured with cathodic-first and anodic-first stimuli at 812.5  $\mu\text{A}$  (producing a loud sensation). The two raw averages are shown in Figure 6 (left column, lower two traces). Each is heavily contaminated by the artifact baseline recovery. Artifact templates were then measured with intensities of 100  $\mu\text{A}$  (subthreshold) and 200  $\mu\text{A}$  (barely audible). The two artifact templates were scaled by 8.125 and 4.0625 respectively to correspond to the intensity used for recording the EPs. The scaled templates are shown superimposed at the top of the left column. In contrast to the templates derived with masking (Figure 3, top of left column), these templates contain no obvious biological component. The correspondence between the two templates confirms the linearity upon which the scaling is predicated. Finally, the 200  $\mu\text{A}$  template was subtracted from the anodic-first average and added to the cathodic-first average to produce the individual responses in the right column. For comparison the response computed with the alternation method is shown at the top of the right column. This waveform is the sum of the two raw averages in the left column. The different individual responses confirm that both the latency and the magnitude of the EP depend upon the stimulus polarity.

*b) Recordings from the Stimulating Electrode*

A remaining objective of this effort is to establish the capability to record EP signals from the same electrode (*i.e.* at the same site) through which the stimulus current is delivered. All of the basic advances described above of a gated, high-bandwidth stimulator in combination with a low-noise, fast-recovery recording amplifier may allow direct recording of EP responses from a stimulated electrode. Studies are in progress to assess the equipment performance under these demanding circumstances and to determine the extent to which electrochemically-generated, post-stimulus after potentials at the electrode interface may contaminate neural potential recordings. Such after potentials will likely be non-linear, and perhaps time-variant. Further modifications to the recording equipment may be needed to provide rapid connect/disconnect to the stimulated electrodes.

A future report will detail further progress with both single polarity stimulation and recording from the stimulated electrode.

### **III. Plans for the Next Quarter**

Our plans for the next quarter include the following:

- Completion of studies with subject ME2, for the period of October 27 to November 14 (see Introduction).
- Studies with Ineraid subjects SR9, SR15 and SR16, principally to evaluate speech reception performance with their portable Innsbruck/RTI processors, following six months of daily use for each subject. The studies also will include measures of channel interaction using recordings of intracochlear evoked potentials, as in prior studies with other subjects. Intracochlear EPs also will be recorded for stimuli used in prior psychophysical studies of pitch scaling for subjects SR15 and SR16 (such recordings already have been made for subject SR9). Additional studies for all three subjects will include (a) measures of stimulus levels corresponding to threshold and most comfortable loudness in the context of multichannel stimulation; (b) comparison of speech processors using mapping functions derived from those measures versus speech processors using mapping functions derived from standard single-channel measures of threshold and MCL; (c) evaluation of proportional reductions in target thresholds across channels in deriving mapping functions; (d) evaluation of "n-of-m" processors; and (e) evaluation of speech processors using relatively high rates of stimulation.
- Ongoing studies with Ineraid subject SR2 (usually one morning per week). Studies anticipated for the next quarter include investigation of effects of various "conditioner" stimuli, such as high rate pulse trains with uniform pulse amplitudes, on the neural representations and perception of superposed "deterministic" stimuli, such as a low rate pulse train with pulse amplitudes greater than that of the conditioner. The investigation will include recordings of intracochlear evoked potentials and psychophysical measures of threshold, loudness growth functions, and frequency (or rate) scaling.
- Resumption of studies with one or more patients implanted with the Clarion device. The studies will include comparisons among (a) compressed analog (CA) processors using the "enhanced bipolar" electrode configuration of the recently modified Clarion implant, (b) CIS processors using monopolar electrodes in the implant, (c) CA processors using monopolar electrodes, and (d) CIS processors using enhanced bipolar electrodes. All processors will use the same number of channels. The processors will be implemented and applied using our laboratory speech processor system and fitting procedures.
- Continued preparation for studies with patients implanted with CI24M devices on both sides.
- Possible initiation of studies with one or more of those patients, depending on the schedule for the implant operations at the University of Iowa and our readiness for the studies.
- Continued studies with subject NU-4, a local patient with standard transcutaneous Nucleus implants on both sides.
- Continued analysis of speech reception and evoked potential data from prior studies.
- Continued preparation of manuscripts for publication.

### **IV. Acknowledgments**

We thank subjects ME1, ME2, SR2, SR3, and SR10 for their participation in the studies of this quarter.

---

# Appendix 1. Summary of Reporting Activity for this Quarter

Reporting activity for the last quarter, covering the period of August 1 through October 31, 1997, included the following:

## Papers

Wilson BS: The future of cochlear implants. *British Journal of Audiology* **31**: 205-225, 1997 (invited guest editorial in celebration of the 30<sup>th</sup> anniversary of the journal).

Lawson DT, Wilson BS, Finley CC, Zerbi M, Cartee LA, Roush PA, Farmer JC Jr, Tucci DL: Cochlear implant studies at Research Triangle Institute and Duke University Medical Center. *Scandinavian Audiology* **26** (Suppl. 46): 50-64, 1997.

## Invited Presentations

Wilson BS, Finley CC, Zerbi M, Lawson DT, van den Honert C: Representations of temporal information in responses of the human auditory nerve to electrical stimuli. *1997 Conference on Implantable Auditory Prostheses*, Pacific Grove, CA, August 17-21, 1997.

Finley CC, Wilson BS, van den Honert C: Fields and EP responses to electrical stimulation: Spatial distributions, electrode interactions and regional differences along the tonotopic axis. *1997 Conference on Implantable Auditory Prostheses*, Pacific Grove, CA, August 17-21, 1997.

Lawson DT, Wilson BS, Zerbi M, Finley CC: Design differences and parametric adjustments among CIS and related processors. *1997 Conference on Implantable Auditory Prostheses*, Pacific Grove, CA, August 17-21, 1997.

Wilson BS: Speech processors for auditory prostheses. *28<sup>th</sup> Annual Neural Prosthesis Workshop*, Bethesda, MD, October 15-17, 1997.

## Chaired Conference

Skinner MW (Chair), Finley CC (Co-Chair): *1997 Conference on Implantable Auditory Prostheses*, Pacific Grove, CA, August 17-21, 1997.

## Chaired Sessions

Blamey P (Discussion Leader), James C (Discussion Co-Leader), Lawson DT (Discussion Co-Leader): Focus group on "Binaural stimulation -- opportunities and limitations." *1997 Conference on Implantable Auditory Prostheses*, Pacific Grove, CA, August 17-21, 1997.

Wilson BS (Discussion Leader), Böex-Spano C (Discussion Co-Leader), Svirsky M (Discussion Co-Leader): Focus group on "Issues in speech processor design." *1997 Conference on Implantable Auditory Prostheses*, Pacific Grove, CA, August 17-21, 1997.